Biophysical Journal Volume 109 July 2015 164–172

Article

Predicting First Traversal Times for Virions and Nanoparticles in Mucus with Slowed Diffusion

Austen M. Erickson,[1] Bruce I. Henry,[1] John M. Murray,[1] Per Johan Klasse,[2] and Christopher N. Angstmann[1,*]
[1]School of Mathematics and Statistics, UNSW Australia, Sydney, New South Wales, Australia; and [2]Department of Microbiology and Immunology, Weill Cornell Medical College, Cornell University, New York, New York

ABSTRACT Particle-tracking experiments focusing on virions or nanoparticles in mucus have measured mean-square displacements and reported diffusion coefficients that are orders of magnitude smaller than the diffusion coefficients of such particles in water. Accurate description of this subdiffusion is important to properly estimate the likelihood of virions traversing the mucus boundary layer and infecting cells in the epithelium. However, there are several candidate models for diffusion that can fit experimental measurements of mean-square displacements. We show that these models yield very different estimates for the time taken for subdiffusive virions to traverse through a mucus layer. We explain why fits of subdiffusive mean-square displacements to standard diffusion models may be misleading. Relevant to human immunodeficiency virus infection, using computational methods for fractional subdiffusion, we show that subdiffusion in normal acidic mucus provides a more effective barrier against infection than previously thought. By contrast, the neutralization of the mucus by alkaline semen, after sexual intercourse, allows virions to cross the mucus layer and reach the epithelium in a short timeframe. The computed barrier protection from fractional subdiffusion is some orders of magnitude greater than that derived by fitting standard models of diffusion to subdiffusive data.

INTRODUCTION

Biological hydrogels, such as mucus, are ubiquitous in the human body and they play a vital role in microscopically regulating particle transport (1). For example, specially prepared nanoparticles may pass through mucus, but in general their movement is obstructed (2–4). Virions of different infections have been shown to be trapped or to pass through mucus to varying degrees, partly in accordance with their size (2–9). In particular, normal, acidic cervicovaginal mucus greatly hinders the movement of virions of herpes simplex virus (HSV) (8) and human immunodeficiency virus (HIV) (10), whereas mucus that is neutralized by semen deposited during coitus or by bacterial vaginosis provides a much less effective barrier against the same virions (10,11). Many experiments focused on particle tracking in mucus, or in simulated biological hydrogels, show subdiffusive behavior (2,4,6,10,12,13) or greatly slowed diffusive behavior (14–17).

The efficacy of hydrogels in providing such a barrier against infection is an important area of study (1,16). Fundamental to this is an understanding of particle diffusion in these systems. Single- and multiple-particle tracking experiments are frequently used to analyze the behavior of particle diffusion through mucus and gels (2–4,6,10,12,14–16). Typical results are in the form of two-dimensional images (and, less commonly, three-dimensional images (12)), which can be used to find trajectories for individual particles. Single-particle tracking experiments make it possible to measure the mean-square displacement of the particles, and many studies infer diffusion coefficients from this (12,18). In standard diffusion, the mean-square displacement of diffusing particles scales as a linear function of time, but in more general models of diffusion such as time-scaled diffusion and fractional subdiffusion, the mean-square displacement scales sublinearly with time. In experimental observations, there is often a large amount of noise in measurements of mean-square displacements, leading to different possible interpretations. Moreover, the means are sometimes calculated as ensemble averages over many particle trajectories, sometimes as time averages over a single-particle trajectory, and sometimes as a combination of the two. The ensemble and time averages are equivalent in standard diffusion, but they are different in time-scaled diffusion and fractional subdiffusion (19). A better understanding of the methods to be applied in particle diffusion through gels is therefore needed.

In the Materials and Methods section, we describe different mathematical models for diffusion, namely, standard diffusion, time-scaled diffusion, and fractional subdiffusion. We present formulae for the first-traversal-time distribution and the associated survival probability for diffusing particles traversing a layer. The first-traversal-time distribution, $f(t)$, gives the probability of a particle arriving at time zero and completely traversing the layer

Submitted December 3, 2014, and accepted for publication May 28, 2015.
*Correspondence: c.angstmann@unsw.edu.au
Editor: Alexander Berezhkovskii.

0006-3495/15/07/0164/9 $2.00
http://dx.doi.org/10.1016/j.bpj.2015.05.034

by the later time t. The survival probability, $S(t)$, is the probability that the particle is still in the layer at time t. For an ensemble of noninteracting particles entering the layer at time $t = 0$, the survival probability represents the proportion of those particles that remain in the layer.

In the Results section, we consider the diffusion of HIV virions in human cervicovaginal mucus. Most of the models for the transport theory of HIV virions, including diffusion across layers, assume standard diffusion (20,21). We use data from experimental observations of mean-square displacements relevant to this problem for three different diffusion models, standard diffusion with an effective diffusion coefficient, time-scaled diffusion, and fractional subdiffusion. We calculate traversal-time statistics based on each of the models. There are large variations in the traversal-time statistics depending on which model is used. Traversal times calculated from a subdiffusive model reveal that the motion of virions is greatly hindered by the presence of acidic mucus. This calculation holds the promise that a thin layer of mucus is thus capable of providing an effective barrier against particle transport.

MATERIALS AND METHODS

In this section, we are interested in calculations relating to the time it takes a particle governed by a particular diffusion process to traverse a layer. For each of the mathematical diffusion models—standard diffusion, time-scaled diffusion, and fractional subdiffusion—we determine the survival probability, $S(t)$, for particles initially localized at a boundary, $x = 0$, to be in the domain $0 \le x \le h$ at a later time t, given that $x = h$ is an absorbing boundary. Fig. 1 is a schematic representation of an initial innoculum of virions entering a mucus layer with absorption at the epithelium. The analysis in this article could be extended to multilayer models taking into account the explicit arrival times of particles and dependent on the different characteristics of the layers. An analagous process could be applied for an axisymmetric three-dimensional model representing the entire vaginal mucosa.

The survival probability is calculated using

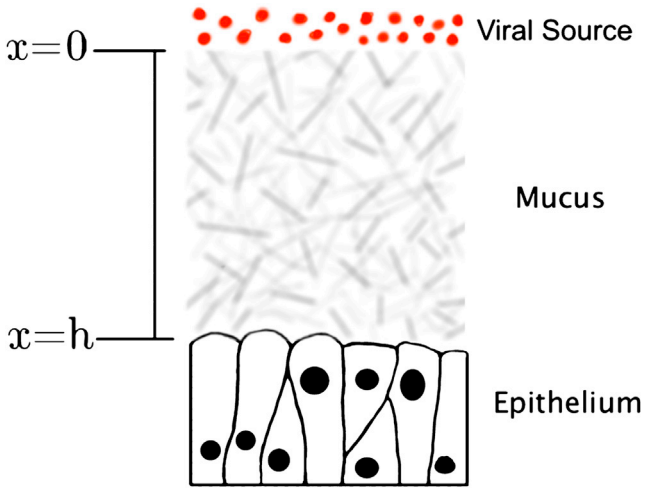

FIGURE 1 Schematic representation of the geometry of the model system for diffusive transport of virions across a mucus layer with an absorbing boundary at the epithelium. To see this figure in color, go online.

$$S(t) = \int_0^h \rho(x,t)dx,$$

where $\rho(x,t)$ is the probability distribution for the position of the particle in the domain at time t. The first-traversal-time distribution can then be found from

$$f(t) = -\frac{\partial S}{\partial t}.$$

Standard diffusion

A mathematical description of the physical process that underlies standard diffusion is Brownian motion (Bm). This can be derived as the diffusion limit of a standard random walk. A standard random walk, in one space dimension, is the process where a walking particle, at each time step, will step to the left or right with equal probability. The diffusion limit is found by taking the length of the spatial and time steps simultaneously to zero (22). The standard diffusion equation provides a model for random motion of the particle in a spatially homogenous medium.

For a particle undergoing Bm, the evolution of the probability density, $\rho(x,t)$, is governed by a diffusion equation. In one dimension, this is given by

$$\frac{\partial \rho}{\partial t} = D\frac{\partial^2 \rho}{\partial x^2}, \tag{1}$$

where D is the diffusion coefficient dependent on physical properties of the diffusing particle and the environment. In this Gaussian process, if two particles have the same diffusion coefficient, D, then all their transport properties are equivalent.

The fundamental solution of the diffusion equation is given by

$$\rho(x,t) = \frac{1}{\sqrt{4\pi D t}}\exp\left(-\frac{x^2}{4Dt}\right).$$

The mean-square displacement is then given by

$$\langle x^2 \rangle = 2Dt, \tag{2}$$

where the average is an ensemble average. The first-traversal-time statistics are found by solving the diffusion equation (Eq. 1) subject to a zero-flux boundary at $x = 0$,

$$\frac{\partial \rho}{\partial x}(0,t) = 0, \tag{3}$$

and an absorbing boundary at $x = h$,

$$\rho(h,t) = 0. \tag{4}$$

An infinite-series solution to this equation can be found using the standard method of separation of variables. Applying the boundary conditions above, we obtain the solution

$$\rho_{\mathrm{Bm}}(x,t) = \frac{2}{h}\sum_{n=0}^{\infty}\left[\exp\left(-\left(\frac{(2n+1)\pi}{2h}\right)^2 Dt\right) \times \cos\left(\frac{(2n+1)\pi}{2h}x\right)\right]. \tag{5}$$

This is not normalized for all time, because there is an absorbing boundary condition at $x = h$. The survival function is the integral of this solution over the spatial domain,

$$S_{\mathrm{Bm}}(t) = \frac{4}{\pi}\sum_{n=0}^{\infty}\left[\exp\left(-\left(\frac{(2n+1)\pi}{2h}\right)^2 Dt\right)\frac{(-1)^n}{2n+1}\right]. \tag{6}$$

The first-traversal-time distribution is the time derivative of the survival function,

$$f_{\mathrm{Bm}}(t) = \frac{D\pi}{h^2}\sum_{n=0}^{\infty}\left[\exp\left(-\left(\frac{(2n+1)\pi}{2h}\right)^2 Dt\right) \times (2n+1)(-1)^n\right]. \tag{7}$$

The median traversal time, defined as the time at which the survival function is equal to one-half, can readily be calculated as a function of the physical parameters D and h. To do this, we define the rescaled survival function, $\widehat{S}_{\mathrm{Bm}}(Dt/h^2) = S_{\mathrm{Bm}}(t)$. The time at which $S_{\mathrm{Bm}}(t)$ is equal to a half, τ_{Bm}, is given by

$$\tau_{\mathrm{Bm}} = \frac{h^2}{D}\widehat{S}^{-1}_{\mathrm{Bm}}\left(\frac{1}{2}\right). \tag{8}$$

By numerically inverting Eq. 8. we find that $\widehat{S}^{-1}_{\mathrm{Bm}}(1/2) = 0.378748$; this is independent of D and h.

The same rescaling applies to the calculation of the mean first transit time, yielding

$$\langle t\rangle = \frac{h^2}{D}s^*, \tag{9}$$

where

$$s^* = \int_0^{\infty} s\widehat{f}_{\mathrm{Bm}}(s)ds, \tag{10}$$

with $s = (Dt/h^2)$ and

$$\widehat{f}_{\mathrm{Bm}}(s) = \frac{h^2}{D}f_{\mathrm{Bm}}(t). \tag{11}$$

Note that s^* is independent of h and D and is equal to the mean first transit time when $h = 1$ and $D = 1$, so that $s^* = 1/2$.

Time-scaled diffusion

In the standard diffusion equation the mean-square displacement scales linearly with time, in contradiction to many experimental measurements. Anomalous scaling, which is not linear with time, can be obtained from a diffusion equation with the diffusion constant replaced by an effective time-dependent diffusion coefficient. The time rescaling models an increasing propensity for a diffusing particle to become trapped and restricted in its motion. The evolution of the probability density in this time-scaled diffusion equation is governed by

$$\frac{\partial\rho}{\partial t} = \alpha t^{\alpha-1}D\frac{\partial^2\rho}{\partial x^2}, \tag{12}$$

so that there is now a power-law time-dependent diffusion coefficient (23),

$$D(t) = \alpha t^{\alpha-1}D. \tag{13}$$

In free space, without boundary conditions, the solution to this equation matches the probability density function for fractional Brownian motion (24–27). However, with the introduction of boundary conditions, the time-scaled diffusion model is no longer a valid model of fractional Brownian motion (19,25,28), and it provides a model for subdiffusion that can be studied in its own right. Like the standard diffusion equation, the time-scaled diffusion equation can be derived as the diffusion limit of a random walk. In this case, at each time step, the random-walking particle steps to either the left or the right with equal probability, or it remains at the same location; the probability of remaining at the same location increases with time. The solution for time-scaled diffusion can be obtained from the solution for standard diffusion (25) by employing a deterministic rescaling in time, replacing t with t^α where $\alpha\in(0, 1)$ is a scaling exponent. This is also true for the mean-square displacement, which thus scales sublinearly with time, i.e., $\langle x^2\rangle = 2Dt^\alpha$. This process is essentially a fitting mechanism that may be useful in approximating true physical processes (19,29).

With the boundary conditions given by Eqs. 3 and 4, and using a deterministic time rescaling in Eq. 5. we obtain

$$\rho_{\mathrm{sBm}}(x,t) = \frac{2}{h}\sum_{n=0}^{\infty}\left[\exp\left(-\left(\frac{(2n+1)\pi}{2h}\right)^2 Dt^\alpha\right) \times \cos\left(\frac{(2n+1)\pi}{2h}x\right)\right]. \tag{14}$$

This then can be integrated over the spatial domain to give the survival function,

$$S_{\mathrm{sBm}}(t) = \frac{4}{\pi}\sum_{n=0}^{\infty}\left[\exp\left(-\left(\frac{(2n+1)\pi}{2h}\right)^2 Dt^\alpha\right)\frac{(-1)^n}{2n+1}\right]. \tag{15}$$

After differentiating with respect to time, we obtain the first-traversal-time distribution,

$$f_{\mathrm{sBm}}(t) = t^{\alpha-1}\frac{\alpha D\pi}{h^2}\sum_{n=0}^{\infty}\left[\exp\left(-\left(\frac{(2n+1)\pi}{2h}\right)^2 Dt^\alpha\right) \times (2n+1)(-1)^n\right], \tag{16}$$

which recovers the result for standard diffusion when $\alpha = 1$.

Similar to the case of standard diffusion, we can derive scaling relations for the mean and median traversal times. Again we can define the rescaled survival function, $\widehat{S}_{\mathrm{sBm}}(Dt^\alpha/h^2) = S_{\mathrm{sBm}}(t)$. The time at which $S_{\mathrm{sBm}}(t)$ is equal to a half, τ_{sBm}, is given by

$$\tau_{\mathrm{sBm}} = \left(\frac{h^2}{D}\widehat{S}^{-1}_{\mathrm{sBm}}\left(\frac{1}{2}\right)\right)^{\frac{1}{\alpha}}. \tag{17}$$

As this must limit to the standard case when $\alpha = 1$, we can see that $\widehat{S}^{-1}_{\mathrm{sBm}}(1/2) = \widehat{S}^{-1}_{\mathrm{Bm}}(1/2) = 0.378748$.

The same rescaling applies to the calculation of the mean first transit time, yielding

$$\langle t\rangle = \left(\frac{h^2}{D}s^*\right)^{\frac{1}{\alpha}}, \tag{18}$$

where again $s^* = (1/2)$.

Fractional subdiffusion

The evolution equation for the probability density function for particles undergoing fractional subdiffusion is given by

$$\frac{\partial \rho}{\partial t} = {}_0D_t^{1-\alpha}\frac{\partial^2 \rho}{\partial x^2}, \tag{19}$$

where

$${}_0D_t^{1-\alpha}y(x,t) = \frac{1}{\Gamma(\alpha)}\frac{\partial}{\partial t}\int_0^t \frac{y(x,t')}{(t-t')^{1-\alpha}}dt'$$

is the Riemann-Liouville fractional time derivative of the function $y(x,t)$ (30). The fractional subdiffusion model can be derived as the diffusion limit of a continuous-time random walk (CTRW). CTRWs are a generalization of the random walk in which the particle undergoes random jumps, drawn from a jump-length probability density, after waiting random times, drawn from a waiting-time probability density (31). If the jump-length density has finite variance and the waiting-time density has a finite first moment, then the diffusion limit of the CTRW recovers the standard diffusion equation. However, if the jump-length density has finite variance but the waiting-time density has a power-law tail, with an infinite first moment, then the diffusion limit of the CTRW recovers a time fractional diffusion equation (30). CTRWs with power-law waiting times are well suited for modeling subdiffusion from particle motion with traps and obstacles. The fractional subdiffusion model is nonergodic and the mean-square displacement scales as a sublinear power law in time,

$$\langle x^2 \rangle = 2D_\alpha t^\alpha,$$

where D_α is a fractional diffusion coefficient that is different for different α.

The solution to the fractional subdiffusion equation can be found from the solution to the standard diffusion equation by performing a stochastic time transformation. This is done by time-subordinating the solution of the standard diffusion equation using an inverse-alpha stable Levy subordinator (32). The time subordination of an exponential function, e^{-kt^α}, is given by $E_\alpha(-kt^\alpha)$, where $E_\alpha(z)$ is a Mittag-Leffler function (33),

$$E_\alpha(z) = \sum_{k=0}^{\infty}\frac{z^k}{\Gamma(1+\alpha k)}.$$

Hence, the probability density function for fractional subdiffusion is simply found by replacing the exponential function in Eq. 14. with a Mittag-Leffler function. This yields

$$\rho_{\mathrm{CTRW}}(x,t) = \frac{2}{h}\sum_{n=0}^{\infty}\left[E_\alpha\left(-\left(\frac{(2n+1)\pi}{2h}\right)^2 D_\alpha t^\alpha\right) \times \cos\left(\frac{(2n+1)\pi}{2h}x\right)\right]. \tag{20}$$

Integrating over the spatial domain gives the survival function,

$$S_{\mathrm{CTRW}}(t) = \frac{4}{\pi}\sum_{n=0}^{\infty}\left[E_\alpha\left(-\left(\frac{(2n+1)\pi}{2h}\right)^2 D_\alpha t^\alpha\right)\frac{(-1)^n}{2n+1}\right]. \tag{21}$$

This agrees with the first-survival-time distribution derived in Yuste and Lindenberg (34) using a different approach.

The first-traversal-time distribution can now be obtained by differentiating the above expression with respect to time, noting that (33)

$$\frac{dE_\alpha(z)}{dz} = \frac{E_{\alpha,\alpha}(z)}{\alpha},$$

where

$$E_{\alpha,\beta}(z) = \sum_{k=0}^{\infty}\frac{z^k}{\Gamma(\beta+\alpha k)}$$

is a two-parameter Mittag-Leffler function.

We thus obtain

$$f_{\mathrm{CTRW}}(t) = t^{\alpha-1}\frac{D_\alpha \pi}{h^2}\sum_{n=0}^{\infty}\left[E_{\alpha,\alpha}\left(-\left(\frac{(2n+1)\pi}{2h}\right)^2 D_\alpha t^\alpha\right) \times (2n+1)(-1)^n\right]. \tag{22}$$

This first-traversal-time distribution for fractional subdiffusion also recovers the first-traversal-time distribution for standard diffusion when $\alpha = 1$.

Again we can derive scaling relations for the median traversal times, although the mean times are infinite. In this case, the rescaled survival function will be dependent on the value of α, $\widehat{S}_{\mathrm{CTRW}}(Dt^\alpha/h^2) = S_{\mathrm{CTRW}}(t)$. The time at which $S_{\mathrm{CTRW}}(t)$ is equal to one-half, τ_{CTRW}, is given by

$$\tau_{\mathrm{CTRW}} = \left(\frac{h^2}{D}\widehat{S}^{-1}_{\mathrm{CTRW}}\left(\frac{1}{2}\right)\right)^{\frac{1}{\alpha}}. \tag{23}$$

As the value of $\widehat{S}^{-1}_{\mathrm{CTRW}}(1/2)$ depends on α, it needs to be calculated for each value under consideration.

RESULTS

In the analysis above, we obtained algebraic expressions for first-traversal-time distributions for three different models of diffusion, standard diffusion, time-scaled diffusion, and fractional subdiffusion. We now consider numerical evaluations based on these models, to quantify differences in traversal times. The first step is to extract values of the model parameters, the diffusion constant D, and the scaling exponent α, from experimental measurements of mean-square displacements.

Estimates of diffusion coefficients and scaling exponents

In an ideal situation, we would have access to experimental data from a large number of particle trajectories over a long period of time, $[0,T]$. This would enable the computation of the ensemble-averaged mean-square displacement as a function of time, $\langle \Delta x^2(t) \rangle$, and a moving time-averaged mean-square displacement versus time, $\overline{\Delta x_{\mathrm{T}}^2(t)}$. In one space dimension, the latter can be computed from the particle position $x(t)$ as

$$\overline{\Delta x_T^2(t)} = \frac{1}{T-t}\int_0^{T-t} \left(x(t+T') - x(T')\right)^2 dT'.$$

The exponent α can be found as the slope of the line of best fit in a log-log plot of the ensemble-averaged mean-square displacement versus time. If $\langle \Delta x^2(t)\rangle \approx \overline{\Delta x_T^2(t)}$, then the underlying physical process is likely to be Brownian motion if $\alpha \approx 1$, or fractional Brownian motion otherwise. If $\alpha \not\approx 1$ and the ensemble average and moving time average are not in agreement, then the time-rescaled diffusion model or the fractional subdiffusion model should be considered. These models can be distinguished through their probability densities; Gaussian in the case of time-scaled diffusion, and non-Gaussian in the case of fractional subdiffusion (30).

Often a particular model is fitted to experimental data without consideration of the different possible physical processes or associated models. Some experimental studies of diffusion in mucus and simulated mucus assume that the mean-square displacement varies linearly with time, as in Eq. 2, to infer a diffusion coefficient, which may be some orders of magnitude smaller than the diffusion coefficient for diffusion in water (14–17). This will yield a constant in the case of standard diffusion. However if the mean-square displacement varies as a sublinear power of time, then D calculated in this fashion will be time-dependent, or it may yield different constant values based on different observation times. It is straightforward, by minimizing the area between two curves, to show that the straight line of best fit to a power law Ct^α over an interval $[0,\tau]$ is given by

$$y(t) = \frac{6C\tau^{\alpha-1}\alpha}{(1+\alpha)(2+\alpha)}t + 2C\frac{(1-\alpha)\tau^\alpha}{(1+\alpha)(2+\alpha)}.$$

The slope of this line provides an estimate for the diffusion coefficient that varies as a function of the observation time, τ. Explicitly,

$$D(\tau) = \frac{3C\tau^{\alpha-1}\alpha}{(1+\alpha)(2+\alpha)}. \tag{24}$$

This is shown schematically in Fig. 2. In this figure we show plots of $\langle x^2(t)\rangle$ versus t for simulated subdiffusion data corresponding to $D_\alpha = 0.006(\mu m/s^\alpha)$ and $\alpha = 0.3$. The value chosen for D_α in this plot is consistent with the value of $\Gamma = 0.023(\mu m/s^\alpha)$ measured in Boukari et al. (12) for slowly diffusing virions following the scaling relation $\langle \mathrm{MSD}\rangle = \Gamma\tau^\alpha + v^2\tau^2$. The sublinear power law, $2D_\alpha t^\alpha$ (*red curve*), provides an excellent fit to all data over this time. The two straight lines of best fit to this power law, based on the data from the first 5 s (*orange line*) and the first 25 s (*green line*), have slopes $2D = 0.001$ and $2D = 0.0004$, respectively. Note that fitting data from shorter observation times will result in a larger slope and faster apparent diffusion than fitting data from longer observation times.

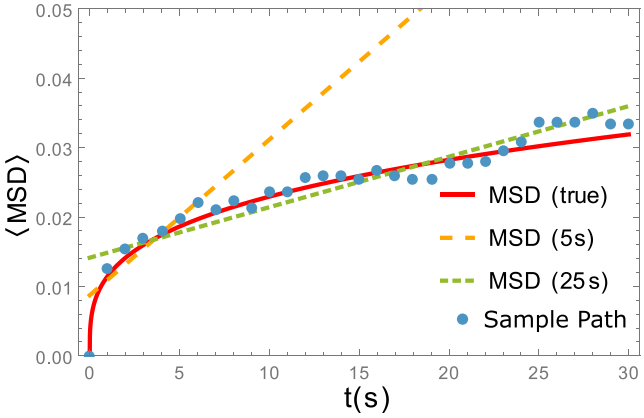

FIGURE 2 Randomly generated sample path characteristic of subdiffusion with $\alpha = 0.3$. Comparisons are made with fits to an ensemble average of such paths based on the best-fit sublinear power law over the 25 s (*red line*), the best-fit straight line for data from the first 5 s (*orange line*), and the best-fit straight line for data from the first 25 s (*green line*). To see this figure in color, go online.

Some experimental studies attempt best fits to a power-law scaling and then use this to infer a time-dependent diffusion coefficient (19,25,29). The identification of a time-dependent diffusion coefficient in this manner implicitly assumes a time-scaled diffusion model (29). Fractional subdiffusion and time-scaled diffusion are not ergodic processes, i.e., time averages are not equivalent to ensemble averages. One important consequence of this for experimental analysis is that it would be inappropriate to infer time-dependent diffusion coefficients based on experimental measurements of time-averaged mean-square displacements.

In the following, to make comparisons between the different models, we assume the same diffusion constant, $D_\alpha = 0.006(\mu m/s^\alpha)$, for time-scaled diffusion and fractional diffusion. This value is within the range of reported values from experimental observations of HIV virions in both acidic and neutralized cervicovaginal mucus. The conclusions that we draw from our results are not sensitive to the particular choice of D_α, which justifies our simplification to use the same D_α for different scaling exponents α. Experimental results show considerable individual variation in α, which is also dependent on the pH of cervicovaginal mucus (35). We use a lower bound of $\alpha = 0.3$ in acidic mucus (10,12) and an upper bound of $\alpha = 0.9$ in neutralized cervicovaginal mucus (10). The mucus thickness has been taken to be the approximate thickness of vaginal fluid in vivo, reported as varying greatly around a mean of $50\mu m$ (4,36,37). The geometry for the calculations is shown schematically in Fig. 1. The calculations that we present here are important for determining the time it takes an infectious agent to cross a mucus layer, thus providing information on a lower bound for infection times. Traversal times may also be used to provide rough estimates of the period over which any antiviral protection, such as a microbicide, would need to be effective.

Median first traversal times

The survival functions and first-traversal-time distributions differ greatly depending on the underlying physical process and the associated diffusion model (see Fig. 3). In this figure, we have shown plots of the first-traversal-time distribution and the survival probability function for two different values of α; and for standard diffusion, time-scaled diffusion, and fractional subdiffusion. In the case of standard diffusion, results are shown for two values of the diffusion coefficient, one based on 5 s data and one based on 25 s data, using Eq. 24. These plots reveal that predictions of the traversal-time statistics based on standard diffusion, with effective-diffusion-coefficient approximations, could be orders of magnitude different from those based on time-scaled diffusion and fractional subdiffusion. The results, which are shown for $\alpha = 0.9$ (Fig. 3, *A* and *C*) and $\alpha = 0.8$ (Fig. 3, *B* and *D*), are characteristic of weak subdiffusion, as observed in neutralized cervicovaginal mucus.

Specifically, considering the first 24 h, the model choice makes a large impact on the relative probability of a virion transiting through the mucus layer. The probability that a virus has traversed by time t is equal to the cumulative distribution function (CDF) of the first-traversal-time distribution. This is simply the complement of the survival function, i.e.,

$$F(t) = 1 - S(t). \tag{25}$$

For example, taking $\alpha = 0.9$, $D_\alpha = 0.006$, and a mucus thickness of 50 μm at 12 h, the CDF of the time-scaled Bm (sBm) process is 3.6×10^{-4}, in comparison to fractional diffusion, where the CDF is 9.6×10^{-4}. Thus, a model based on fractional diffusion will result in almost three times as many virions crossing the mucus in the first 12 h. Proportionally, this difference decreases with time: at 24 h, the CDF for the sBm processes is 1.2×10^{-2} and, for fractional diffusion, is 1.7×10^{-2}. Both of these values are orders of magnitude smaller than the Brownian motion values.

A useful measurement that can readily be extracted from the survival function is the median traversal time, defined as the time at which the survival function, $S(t)$, reaches the threshold value of one-half. For the system of virions crossing a mucus layer, this represents the time at which one-half of the virions have successfully crossed the mucus layer. The traversal time will clearly depend on the thickness of the layer. The thickness of the vaginal mucus layer varies greatly around 50μm (36,37). It is estimated to be at least tens of micrometers thick in most areas (3), but can range from completely absent to a few millimeters (4). Hence, biologically relevant systems and their mathematical descriptions must cover a wide range of α and h values. Here, we describe how this variation affects predictions of the median traversal times from the time-scaled diffusion model and the fractional subdiffusion model.

Fig. 4 explores the impact of the various models on median and mean first-traversal times. It can be seen that increasing the exponent α (closer to standard diffusion) results in a decreased median first-traversal time. The effect of subdiffusion is dramatic, with variations over several orders of magnitude from low α compared with standard diffusion ($\alpha = 1$) (Fig. 4 *A*). Under the assumptions of this model, merely a micrometer of acidic mucus ($\alpha = 0.3$) can trap over half of incoming virions for well over a week. However, that same layer of mucus, when neutralized ($\alpha = 0.9$), traps half of incoming virions for less than 2 min. The ratio of median first-traversal times for the CTRW and sBm models is different from 1 for all α<1, with the difference becoming greater at small α (Fig. 4 *B*). For example, this ratio is ~2.5 when $\alpha = 0.3$. Increasing mucus thickness also increases both median and mean first-traversal times (Fig. 4, *C* and *D*). These effects are enormous in acidic

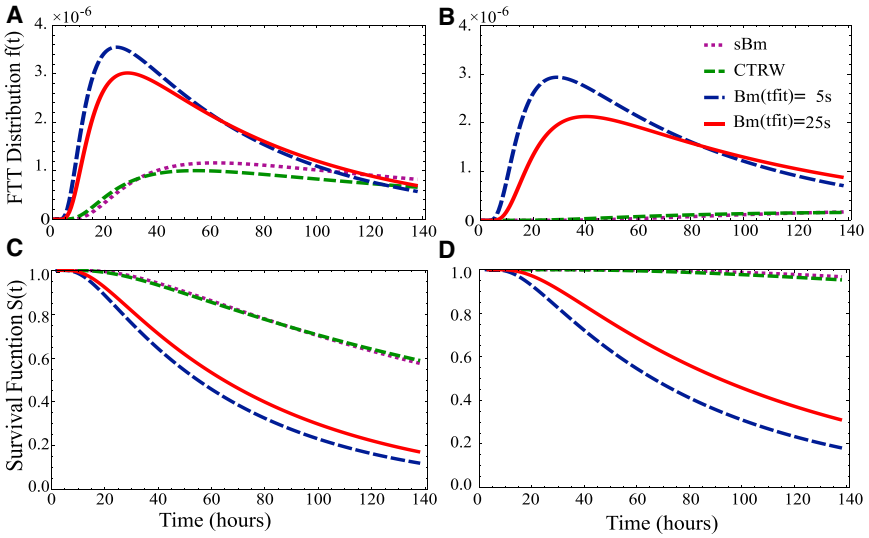

FIGURE 3 Plots of first-traversal-time distributions (*A* and *B*) and survival functions (*C* and *D*) over a mucus layer of thickness $h = 50$ μm. The plots show standard diffusion for two choices of D based on time-scaled diffusion, with $D_\alpha = 0.006(\mu m^2/s^\alpha)$, and fractional subdiffusion, with $D_\alpha = 0.006(\mu m^2/s^\alpha)$, and with diffusion coefficients for Bm approximations calculated from Eq. 31. In (*A*) and (*C*), $\alpha = 0.9$, $D_{5s} = 0.005$, and $D_{25s} = 0.004$, whereas in (*B*) and (*D*), $\alpha = 0.8$, $D_{5s} = 0.004$, and $D_{25s} = 0.003$. To see this figure in color, go online.

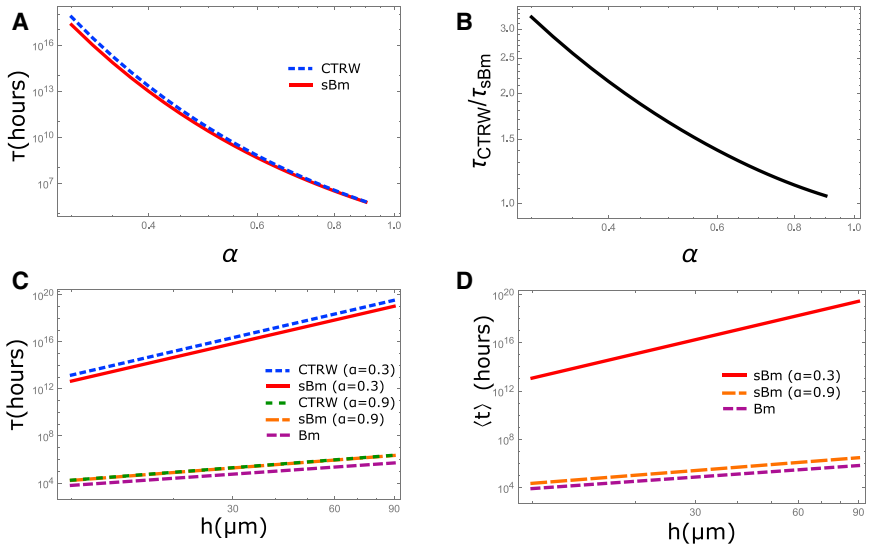

FIGURE 4 Plots of median first-traversal times and mean traversal times in hours (in all instances, $D = 0.006(\mu m^2/s^\alpha)$). (*A*) Log-log plots of the median first-traversal time as a function of α from the CTRW model (*blue dashed line*) and from the time-scaled diffusion model (*red line*). The mucus thickness is taken to be 50 μm. (*B*) Log-log plot of the ratio of the median first-traversal time from the CTRW model to the median first-passage time of the time-scaled diffusion model as a function of α. This ratio does not depend on the diffusivity or the mucus thickness. (*C*) Log-log plots of the median first-traversal time from CTRW $\alpha = 0.3$ (*blue dashed line*), time-scaled diffusion $\alpha = 0.3$ (*red line*), CTRW $\alpha = 0.9$ (*green dashed line*), time-scaled diffusion $\alpha = 0.9$ (*orange dashed line*), and standard diffusion (*purple dashed line*). (*D*) Log-log plots of the mean first-traversal time from time-scaled diffusion $\alpha = 0.3$ (*red line*) and $\alpha = 0.9$ (*orange dashed line*) and standard diffusion (*purple dashed line*). To see this figure in color, go online.

mucus ($\alpha = 0.3$). The anomalous diffusion of mucoadhesive nanoparticles and viruses like HIV can depend on the chemical properties of the medium (10,16), with HIV moving considerably faster through neutralized ($\alpha = 0.9$) than through acidic ($\alpha = 0.3$) mucus. Although the vaginal environment is naturally acidic, after unprotected coitus and ejaculation (and the possible introduction of a sexually transmitted virus), it becomes temporarily neutralized after the deposition of semen (38,39).

DISCUSSION

There have been many experimental studies of virions in mucus that have reported anomalous diffusion based on observations of mean-square displacement as a function of time. The anomalous diffusion is variously characterized by a very small effective diffusion coefficient derived from a linear scaling with time, or by an exponent derived from a sublinear power law scaling with time. Understanding the ramifications of this anomalous diffusion for other transport properties is of vital importance for research on developing preventive measures, i.e., microbicides and vaccines, that act in the earliest stages of infection (40,41). With sufficiently robust particle-tracking data, it would be possible to determine the most likely source of anomalous diffusion and the appropriate corresponding mathematical model. It would also be possible to identify transient anomalous diffusion (23,42,43). These mathematical tests that distinguish between different diffusion models require the comparison of time-averaged data over long continuous particle tracks, and ensemble averages over many particle tracks (44).

The model calculations in this article focus on the rather idealized situation of virions diffusing through a mucus layer, and they ignore all complications arising from the manner in which the virions are delivered to the mucus layer. For example, semen-mucus interactions could greatly increase the concentration of virions that could penetrate the mucus layer.

We have presented first-traversal-time statistics based on different models of diffusion for HIV virions traversing a mucus barrier. The mathematical formulae are relevant for any system of small particles, such as virions or nanoparticles, undergoing trapping-based diffusion across some surface coating, such as mucus or a topical gel. In the application to HIV virions, we use reported experimental results to obtain model parameters for the time-scaled diffusion model and the fractional subdiffusion model, and we assume a mucus layer whose thickness is on the order of micrometers. The median first-traversal time is very sensitive to the anomalous diffusion exponent in these calculations. Low values of the exponent ($\alpha = 0.3$) have been associated with diffusion in normal acidified cervicovaginal mucus. Our estimates of the traversal times in this case are on the order of weeks. Large values of the exponent ($\alpha = 0.9$) have been associated with an increase in the pH of the cervicovaginal mucus, which can occur during coitus because of the alkaline properties of semen (38,39). Our estimates for traversal times in this case are much lower, on the order of minutes.

The clearance time for human cervicovaginal mucus from the female genital tract is on the order of a few hours (3), and the mucus layer is estimated to be tens of micrometers thick (3,4). Our results suggest that under the assumptions of the model, an acidic cervical mucus layer will effectively trap the vast majority of incoming HIV virions. However, a nonacidic neutralized cervicovaginal mucus layer, such as that expected after coitus, will facilitate traversal of the mucus layer, potentially leading to infection of susceptible cells accessible from the epithelial surface. Given that the

explicit model assumptions need to be further experimentally tested, the action of a thin layer of acidic mucus as a potential diffusion barrier should be addressed by experimental studies.

Given the infrequency of HIV infection (as low as 1 in 1000 (45)), there may be several barriers to the establishment of infection. What prevents infection might simply be that too few infectious virions are successfully deposited, that too many are prevented from penetrating the epithelium and subepithelium, or that there are insufficient numbers of target cells there. The extent to which the acidity of cervicovaginal mucus can be maintained postcoitus may contribute to this low infection rate by allowing the mucus to act as a diffusional barrier. The above results are highly sensitive to model assumptions, which must be further investigated using more robust models.

A potentially important aspect is the mechanical effect of coitus on mucus thickness. However, these results are encouraging for the development of microbicides and vaccines designed to block the early events in HIV infection; neutralizing antibodies and other entry inhibitors binding to the virions would have the time window set by diffusion to act before the virus encounters susceptible cells (40,41,46–49). Mathematical models, such as the time-scaled diffusion model and the fractional subdiffusion model, can guide the development of preventative strategies, but it is vital that experimental data be collected and analyzed correctly, with an understanding and knowledge of the model assumptions and limitations.

SUPPORTING MATERIAL

Mathematica code for the calculation of first traversal times is available at http://www.biophysj.org/biophysj/supplemental/S0006-3495(15)00546-9.

AUTHOR CONTRIBUTIONS

B.I.H. and C.N.A. designed the research; A.M.E. and C.N.A. performed the research; A.M.E., B.I.H., J.M.M., P.J.K., B.I.H., and C.N.A. analyzed the data; and A.M.E., B.I.H., J.M.M., P.J.K., B.I.H., and C.N.A. wrote the article.

ACKNOWLEDGMENTS

The authors gratefully acknowledge assistance from an Australian Research Council Grant, DP130100595, funded by the Australian Commonwealth Government. The work of P.J.K. in this area was supported by National Institutes of Health grant R37AI36082.

REFERENCES

1. Lieleg, O., and K. Ribbeck. 2011. Biological hydrogels as selective diffusion barriers. *Trends Cell Biol.* 21:543–551.
2. Lai, S. K., D. E. O'Hanlon, …, J. Hanes. 2007. Rapid transport of large polymeric nanoparticles in fresh undiluted human mucus. *Proc. Natl. Acad. Sci. USA.* 104:1482–1487.
3. Lai, S. K., Y. Y. Wang, and J. Hanes. 2009. Mucus-penetrating nanoparticles for drug and gene delivery to mucosal tissues. *Adv. Drug Deliv. Rev.* 61:158–171.
4. das Neves, J., C. M. Rocha, …, B. Sarmento. 2012. Interactions of microbicide nanoparticles with a simulated vaginal fluid. *Mol. Pharm.* 9:3347–3356.
5. Hida, K., S. K. Lai, …, J. Hanes. 2011. Common gene therapy viral vectors do not efficiently penetrate sputum from cystic fibrosis patients. *PLoS ONE.* 6:e19919.
6. Yang, X., K. Forier, …, H. J. Nauwynck. 2012. Immobilization of pseudorabies virus in porcine tracheal respiratory mucus revealed by single particle tracking. *PLoS ONE.* 7:e51054.
7. Lieleg, O., C. Lieleg, …, K. Ribbeck. 2012. Mucin biopolymers as broad-spectrum antiviral agents. *Biomacromolecules.* 13:1724–1732.
8. Olmsted, S. S., J. L. Padgett, …, R. A. Cone. 2001. Diffusion of macromolecules and virus-like particles in human cervical mucus. *Biophys. J.* 81:1930–1937.
9. Suh, J., M. Dawson, and J. Hanes. 2005. Real-time multiple-particle tracking: applications to drug and gene delivery. *Adv. Drug Deliv. Rev.* 57:63–78.
10. Lai, S. K., K. Hida, …, J. Hanes. 2009. Human immunodeficiency virus type 1 is trapped by acidic but not by neutralized human cervicovaginal mucus. *J. Virol.* 83:11196–11200.
11. Wang, Y.-Y., A. Kannan, …, S. K. Lai. 2014. IgG in cervicovaginal mucus traps HSV and prevents vaginal herpes infections. *Mucosal Immunol.* 7:1036–1044.
12. Boukari, H., B. Brichacek, …, R. Nossal. 2009. Movements of HIV-virions in human cervical mucus. *Biomacromolecules.* 10:2482–2488.
13. Lai, S. K., Y. Y. Wang, …, J. Hanes. 2010. Nanoparticles reveal that human cervicovaginal mucus is riddled with pores larger than viruses. *Proc. Natl. Acad. Sci. USA.* 107:598–603.
14. Lai, B. E., A. R. Geonnotti, …, D. F. Katz. 2010. Semi-solid gels function as physical barriers to human immunodeficiency virus transport in vitro. *Antiviral Res.* 88:143–151.
15. Mahalingam, A., J. I. Jay, …, P. F. Kiser. 2011. Inhibition of the transport of HIV in vitro using a pH-responsive synthetic mucin-like polymer system. *Biomaterials.* 32:8343–8355.
16. Jay, J. I., S. Shukair, …, P. F. Kiser. 2009. Modulation of viscoelasticity and HIV transport as a function of pH in a reversibly crosslinked hydrogel. *Adv. Funct. Mater.* 19:2969–2977.
17. Dawson, M., E. Krauland, …, J. Hanes. 2004. Transport of polymeric nanoparticle gene carriers in gastric mucus. *Biotechnol. Prog.* 20:851–857.
18. Qian, H., M. P. Sheetz, and E. L. Elson. 1991. Single particle tracking. Analysis of diffusion and flow in two-dimensional systems. *Biophys. J.* 60:910–921.
19. Sokolov, I. M. 2012. Models of anomalous diffusion in crowded environments. *Soft Matter.* 8:9043–9052.
20. Geonnotti, A. R., and D. F. Katz. 2006. Dynamics of HIV neutralization by a microbicide formulation layer: biophysical fundamentals and transport theory. *Biophys. J.* 91:2121–2130.
21. Lai, B. E., M. H. Henderson, …, D. F. Katz. 2009. Transport theory for HIV diffusion through in vivo distributions of topical microbicide gels. *Biophys. J.* 97:2379–2387.
22. Kac, M. 1947. Random walk and the theory of Brownian motion. *Am. Math. Mon.* 54:369–391.
23. Thiel, F., F. Flegel, and I. M. Sokolov. 2013. Disentangling sources of anomalous diffusion. *Phys. Rev. Lett.* 111:010601.
24. Mandelbrot, B., and J. van Ness. 1968. Fractional Brownian motions, fractional noises and applications. *SIAM Rev. Soc. Ind. Appl. Math.* 10:422–437.
25. Lim, S. C., and S. V. Muniandy. 2002. Self-similar Gaussian processes for modeling anomalous diffusion. *Phys. Rev. E Stat. Nonlin. Soft Matter Phys.* 66:021114.

26. Wang, K. G., and C. W. Lung. 1990. Long-time correlation-effects and fractal Brownian-motion. *Phys. Lett. A.* 151:119–121.
27. Maccone, C. 1981. Time rescaling and Gaussian properties of the fractional Brownian motions. *Nuovo Cim. B.* 65:259–271.
28. Jeon, J. H., A. V. Chechkin, and R. Metzler. 2011. First passage behaviour of fractional Brownian motion in two-dimensional wedge domains. *Europhys. Lett.* 94:20008.
29. Thiel, F., and I. M. Sokolov. 2014. Scaled Brownian motion as a mean-field model for continuous-time random walks. *Phys. Rev. E Stat. Nonlin. Soft Matter Phys.* 89:012115.
30. Metzler, R., and J. Klafter. 2000. The random walk's guide to anomalous diffusion: a fractional dynamics approach. *Phys. Rep.* 339:1–77.
31. Montroll, E. W., and G. H. Weiss. 1965. Random walks on lattices. II. *J. Math. Phys.* 6:167–181.
32. Magdziarz, M., and K. Weron. 2006. Anomalous diffusion schemes underlying the Cole-Cole relaxation: the role of the inverse-time α-stable subordinator. *Physica A.* 367:1–6.
33. Haubold, H. J., A. M. Mathai, and R. K. Saxena. 2011. Mittag-leffler functions and their applications. *J. Appl. Math.* 2011:298628.
34. Yuste, S. B., and K. Lindenberg. 2004. Comment on "mean first passage time for anomalous diffusion". *Phys. Rev. E Stat. Nonlin. Soft Matter Phys.* 69:033101, discussion 033102.
35. Shukair, S. A., S. A. Allen, …, T. J. Hope. 2013. Human cervicovaginal mucus contains an activity that hinders HIV-1 movement. *Mucosal Immunol.* 6:427–434.
36. Chen, A., S. A. McKinley, …, S. K. Lai. 2014. Transient antibody-mucin interactions produce a dynamic molecular shield against viral invasion. *Biophys. J.* 106:2028–2036.
37. McKinley, S. A., A. Chen, …, S. K. Lai. 2014. Modeling neutralization kinetics of HIV by broadly neutralizing monoclonal antibodies in genital secretions coating the cervicovaginal mucosa. *PLoS ONE.* 9:e100598.
38. Fox, C. A., S. J. Meldrum, and B. W. Watson. 1973. Continuous measurement by radio-telemetry of vaginal pH during human coitus. *J. Reprod. Fertil.* 33:69–75.
39. Tevi-Bénissan, C., L. Bélec, …, G. Grésenguet. 1997. In vivo semen-associated pH neutralization of cervicovaginal secretions. *Clin. Diagn. Lab. Immunol.* 4:367–374.
40. Haase, A. T. 2010. Targeting early infection to prevent HIV-1 mucosal transmission. *Nature.* 464:217–223.
41. Haase, A. T. 2011. Early events in sexual transmission of HIV and SIV and opportunities for interventions. *Annu. Rev. Med.* 62:127–139.
42. Meroz, Y., I. M. Sokolov, and J. Klafter. 2013. Test for determining a subdiffusive model in ergodic systems from single trajectories. *Phys. Rev. Lett.* 110:090601.
43. Berezhkovskii, A. M., L. Dagdug, and S. M. Bezrukov. 2014. Discriminating between anomalous diffusion and transient behavior in microheterogeneous environments. *Biophys. J.* 106:L09–L11.
44. Meroz, Y., and I. M. Sokolov. 2015. A toolbox for determining subdiffusive mechanisms. *Phys. Rep.* 573:1–29.
45. Wawer, M. J., R. H. Gray, …, T. C. Quinn. 2005. Rates of HIV-1 transmission per coital act, by stage of HIV-1 infection, in Rakai, Uganda. *J. Infect. Dis.* 191:1403–1409.
46. Klasse, P. J., R. Shattock, and J. P. Moore. 2008. Antiretroviral drug-based microbicides to prevent HIV-1 sexual transmission. *Annu. Rev. Med.* 59:455–471.
47. Hope, T. J. 2011. Moving ahead an HIV vaccine: to neutralize or not, a key HIV vaccine question. *Nat. Med.* 17:1195–1197.
48. Burton, D. R., R. Ahmed, …, R. Wyatt. 2012. A blueprint for HIV vaccine discovery. *Cell Host Microbe.* 12:396–407.
49. Koff, W. C., D. R. Burton, …, S. A. Plotkin. 2013. Accelerating next-generation vaccine development for global disease prevention. *Science.* 340:1232910.